Shape abnormalities of caudate nucleus in schizotypal personality disorder

James J. Levitt [a,b,*], Martin Styner [d], Marc Niethammer [d], Sylvain Bouix [b], Min-Seong Koo [e], Martina M. Voglmaier [a,f], Chandlee C. Dickey [a,b], Margaret A. Niznikiewicz [a,b], Ron Kikinis [c], Robert, W. McCarley [a], Martha E. Shenton [a,b,c]

[a] Laboratory of Neuroscience, Department of Psychiatry, Veterans Affairs Boston Healthcare System, Brockton Division, Harvard Medical School, Brockton, MA, USA
[b] Psychiatry Neuroimaging Laboratory, Department of Psychiatry, Brigham and Women's Hospital, Harvard Medical School, Boston, MA, USA
[c] Surgical Planning Laboratory, Magnetic Resonance Imaging Division, Department of Radiology, Brigham and Women's Hospital, Harvard Medical School, Boston, MA, USA
[d] Department of Computer Science and Department of Psychiatry, University of North Carolina, Chapel Hill, NC, USA
[e] College of Medicine, Kwandong University, Seoul, Korea
[f] Department of Psychiatry, Cambridge Health Alliance, Cambridge, MA, USA

ARTICLE INFO

ABSTRACT

Background: Previously, we reported abnormal volume and global shape in the caudate nucleus in schizotypal personality disorder (SPD). Here, we use a new shape measure which importantly permits local in addition to global shape analysis, as well as local correlations with behavioral measures.

Methods: Thirty-two female and 15 male SPDs, and 29 female and 14 male normal controls (NCLs), underwent brain magnetic resonance imaging (MRI). We assessed caudate shape measures using spherical harmonic-point distribution model (SPHARM-PDM) methodology.

Results: We found more pronounced global shape differences in the right caudate in male and female SPD, compared with NCLs. Local shape differences, principally in the caudate head, survived statistical correction on the right. Also, we performed correlations between local surface deformations with clinical measures and found significant correlations between local shape deflated deformations in the anterior medial surface of the caudate with verbal learning capacity in female SPD.

Conclusions: Using SPHARM-PDM methodology, we found both global and local caudate shape abnormalities in male and female SPD, particularly right-sided, and largely restricted to limbic and cognitive anterior caudate. The most important and novel findings were bilateral statistically significant correlations between local surface deflations in the anterior medial surface of the head of the caudate and verbal learning capacity in female SPD. By extension, these local caudate correlation findings implicate the ventromedial prefrontal cortex (vmPFC), which innervates that area of the caudate, and demonstrate the utility of local shape analysis to investigate the relationship between specific subcortical and cortical brain structures in neuropsychiatric conditions.

© 2008 Published by Elsevier B.V.

1. Introduction

One of the key circuits in the brain, which connects prefrontal cortical and subcortical regions, is the frontal-striatal-thalamic (FST) circuit. Here, we explore in SPD subjects a key subcortical component of this circuit, the caudate nucleus, using shape analyses to provide both global and local information. Abnormalities in any of the core components of the FST circuit may functionally "disconnect" the overall circuit, resulting in behavioral syndromes that resemble syndromes resulting from pathology to the prefrontal cortex, itself (e.g., Bhatia and Marsden, 1994; Calabresi et al., 1997; Cummings, 1993; Levitt et al., 2002). The caudate

is one of these core components, which if abnormal, can disrupt the flow of information through the FST loops.

Haber et al., (2000), derived from their work in adult macaques, proposed that the striatum can be divided into 3 functional subregions based on the afferent inputs received from the frontal cortex and from the substantia nigra. Furthermore, these frontal projections to the striatum are arranged in a ventromedial to dorsolateral gradient from limbic to cognitive to motor functions. The dorsolateral striatum (the motor region) receives afferent input from motor cortex, primarily from premotor, motor and cingulate motor cortices, the central striatum (the cognitive region) receives afferent input from association (cognitive) cortex, primarily dorsolateral prefrontal cortex, and the ventromedial striatum (the limbic region including the nucleus accumbens) receives afferent input from limbic cortex, primarily from orbital and medial prefrontal cortex. Given the functional heterogeneity of the striatum, a more local and refined level of analysis, such as that provided by our surface based shape analysis, may uncover local caudate group differences. By extension, this may implicate inter-connected specific frontal-subcortical subloop circuits innervating local caudate areas.

We have previously studied the caudate nucleus in SPD in order to avoid the confounding effects of medication and chronicity as these subjects are not overtly psychotic and, hence, do not require neuroleptic treatment or recurrent hospitalizations. Moreover, genetic studies support that SPD is part of the schizophrenia spectrum, (Kendler et al., 1993; Siever et al., 1993) suggesting that pathology found in SPD will be relevant for understanding pathology in schizophrenia. Furthermore, the study of SPD has importance as a way to understand better the pathophysiology of schizophrenia, itself. Siever and Davis (2004) have comprehensively reviewed the ways in which understanding both the shared neurobiological liability of SPD with schizophrenia and the factors protecting SPD subjects from developing features of chronic schizophrenia, including frank psychosis, can help to understand further the pathophysiology of schizophrenia and lead to possible preventive measures. In particular, these authors propose that subjects with SPD, compared with schizophrenics, may have more "frontal reserve capacity" together with reduced subcortical responsiveness of dopamine activity, the latter of which, in turn, makes SPD subjects less vulnerable to the effects of hypofrontality, or what they label as "frontal hypodopaminergia". Such "frontal hypodopaminergia", the authors review, in rodent studies, can lead to subcortical dopamine upregulation. For example, based on research in rodents, it has been hypothesized that decreased prefrontal cortical dopamine levels may result in disinhibition of dopamine neurons that project to the striatum (Akil et al., 2003; Weinberger, 1987). A possible consequence of such neurobiological differences between SPD and schizophrenia, as suggested by Siever and Davis (2004), is that SPD subjects are less prone to developing the frank psychosis and severe deficits in social and cognitive functioning of chronic schizophrenia.

In two prior volumetric studies in neuroleptic-naive male (Levitt et al., 2002) and female (Koo et al., 2006) SPD subjects, compared with matched controls, we found a significant bilateral reduction in caudate nucleus volume. Furthermore, we previously assessed the global shape of the head of the caudate nucleus in male SPD and found a difference between SPD males and controls, lateralized to the right, with correlations in SPD males between global shape and poorer neuropsychological performance (Levitt et al., 2004). Our current surface based shape method (Gerig and Styner, 2001; Shenton et al., 2002; Styner et al., 2004, 2005, 2006) adds the crucial advantage of permitting local as well as a global shape analysis and, furthermore, allows for performing local clinical correlations. We also note that there has been a negative finding for a change in caudate volume in SPD. More specifically, Shihabuddin et al., (2001), found diminished putamen volume, but not caudate volume, in SPD compared to controls. In this study, however, their method for measuring striatal structures differed from our own. In this report, which also examined striatal glucose metabolic rate, the putamen and caudate were measured only on 2 MRI slices, "corresponding to dorsal and ventral levels" and normalized for whole brain volume. Furthermore, in a pilot study by Seidman et al., (1997), using 11 controls and 6 relatives, findings were suggestive of a reduction in putamen, but not caudate volume, in non-psychotic siblings of schizophrenic patients.

In this study, assessing local and global caudate shape in neuroleptic-naive male and female SPD subjects, in whom we have shown bilateral reductions of caudate nucleus volume, we hypothesized the following: (1) local shape surface deflation will be non-uniformly distributed with more pronounced deformation in limbic and cognitive anterior subregions, compared with the motor subregion, of the caudate nucleus in both male and female SPDs; (2) convergent with our prior shape analyses in a male sample, we predict that we will find more local right lateralized shape abnormalities in male SPDs; and, (3) correlations between local caudate shape deformation and clinical measures also will be non-uniformly distributed and will show stronger relationships with anterior regions of the caudate.

2. Methods

2.1. Subjects

Both male and female SPD subjects underwent MRI scanning on a 1.5 Tesla General Electric scanner (GE Medical Systems, Milwaukee, WI). The subjects consisted of 32 female and 15 male SPD subjects, together with 29 female NCLs and 14 male NCLs, respectively. Subject characteristics, the recruitment and diagnostic methods employed by us are described in greater detail in previous studies from our group (Dickey et al., 2000; Koo et al., 2006; Levitt et al., 2004). In brief, SPD and NCLs were interviewed by either a research psychologist or psychiatrist using the SCID-P (First et al., 1995) and the personality disorders version of the SCID (SCID-II) (First et al., 1997). Inclusion criteria were: 1) age between 18–55 years; 2) right-handedness; 2) English as the primary language; 3) no history of neurological disorder (including head trauma with loss of consciousness greater than 2 min); 4) no history of ECT, no drug or alcohol dependence ever or abuse in the last year; and 5) no history of current or past use of neuroleptic medications; 6) no current use of psychotropic medications and no use of medications that might affect MRI such as steroids. Interrater reliability for the diagnosis of SPD, as previously reported, was high (kappa = 0.89, $n = 25$).

NCLs were required not to have a personal or family history (in first degree relatives) of major mental illness or a

personal history of personality disorder. There were no significant group differences in demographic characteristics between male SPD and male control subjects in mean age (38.5 SD 11.0 years vs. 38.0 years SD 10.5 years), number of years of education completed, estimated IQ, or parental socioeconomic status, although personal socioeconomic status did differ ($p<0.01$). Similarly, there were no significant group differences in demographic characteristics between female SPD and female control subjects in mean age (30.0 SD 9.2 years vs. 32.0 years SD 10.5 years), number of years of education completed ($p=0.07$), estimated IQ, or parental socioeconomic status, although as with the male subjects, personal socioeconomic status did differ ($p<0.01$).

Written informed consent was obtained from all male and female subjects, who were the same subjects used in our prior MRI caudate volumetric studies, after they received a complete description of the studies.

2.2. Measures of psychopathology

The cognitive and clinical tests that we previously used and which revealed significant global caudate volume behavior correlations for female SPD subjects were: 1) the California Verbal Learning Test, CVLT (Delis et al., 1987), a measure of verbal learning capacity, 2) the Wisconsin Card Sorting Test (WCST) (Heaton, 1981), a measure of concept formation and set shifting; and, 3) a modified Structured Interview for Schizotypy (SIS; Kendler et al., 1989), appropriate for assessing subtle SPD symptoms. For male SPD subjects the cognitive tests we previously used and which revealed significant global caudate volume behavior correlations were: 1) a delayed alternation spatial working memory task; and, 2) the Controlled Oral Word Association Test, a verbal fluency working memory task (Levitt et al., 2002). In this earlier male SPD study, we used the SANS and SAPS (Andreasen, 1981; Andreasen, 1984) to assess clinical symptoms, which did not yield any significant caudate volume clinical correlations. Here, we reassessed these same correlations but, instead, performed the within group correlations locally, based upon local shape deformation. In order to reduce the probability of type I errors, we restricted our local shape analyses to just those prior global caudate volume behavior correlations which we had previously found to be significant in our studies of global volume of the caudate in male and female SPD.

3. MRI methods

3.1. Image acquisition and post-processing

Images were acquired using a 1.5 Tesla General Electric Scanner (GE Medical Systems, Milwaukee WI). The methodology employed in this study has been described previously in detail (Dickey et al., 2000; Gerig et al., 1992a). Briefly, images were acquired using two pulse sequences. A 3D Fourier Transform Spoiled Gradient-Recalled Acquisition (SPGR) sequence was used to delineate caudate ROIs yielding a series of contiguous 1.5-mm coronal images throughout the brain. The parameters used were: echo time (TE) = 5 ms, repetition time (TR) = 35 ms, one repetition, nutation angle = 45°, field of view = 24 cm, acquisition matrix = 256×256×124, voxel dimensions = 0.9375×0.9375×1.5 mm. Additionally, an axial series of double-echo (proton density and T2 weighted) images was acquired. The imaging parameters used were: echo time (TE) = 30 and 80 ms, repetition time (TR) = 3000 ms, field of view = 24 cm, acquisition matrix = 256×256×108, voxel dimensions = 0.9375×0.9375×3.0 mm. An anisotropic diffusion filter was applied to each set of scans to reduce noise prior to further processing steps (Gerig et al., 1992b). To obtain intracranial contents (ICC), the double echo images were reformatted and registered to the 1.5 mm SGPR images and the resulting image was used to obtain ICC volumes using an iterative expectation-maximization segmentation protocol (Wells et al., 1996). MRI caudate nucleus manual tracing measurements were all performed blind to diagnostic status.

3.2. Anatomical landmarks for the caudate nucleus

The caudate nucleus was measured manually, bilaterally, using our medical image editing software, 3D-slicer (http://www.slicer.org), where we used 3 orthogonal views, as previously described in detail (Levitt et al., 2002). Briefly, the caudate head, body and tail were measured including where the tail bordered the lateral aspect of the atrium of the lateral ventricles. Where the caudate and putamen are joined anteriorly, we separated them by drawing a vertical line from the most ventral point of the internal capsule down to the external capsule, including much of the nucleus accumbens, and forming the inferior-lateral bound of the caudate nucleus. Inter-rater reliability, as previously reported, was high for left and right caudate nucleus ($r_I>0.98$) for male SPD subjects (Levitt et al., 2002) as it was for left ($r_i=0.95$) and right ($r_i=0.94$) caudate nucleus in female SPD subjects (Koo et al., 2006).

3.3. MR shape analysis

Our shape analysis of the manual caudate segmentation runs automatically using the UNC shape analysis tools[1] and is applied to all segmented datasets in the same manner. A detailed description of all steps of the shape description and the statistical analysis is available in Styner et al., (2006). In the first step of the processing, the caudate segmentations are adapted to fill any interior holes, followed by the application of a morphological closing operation and a minimal smoothing operation. The boundary surfaces of the processed segmentations are represented on the sphere in terms of spherical harmonic-based shape descriptions (Brechbuhler et al., 1995), which continuously describe the surfaces by sets of coefficients weighting the spherical harmonic basis functions. The surface correspondence between different surfaces is established by parameter-space rotation based on the first-order expansion of spherical harmonics. This parametric spherical harmonic-based shape description is then uniformly sampled into a set of 1002 surface points, called SPHARM-PDM. Each surface is then spatially aligned to an average caudate template using rigid Procrustes alignment (Bookstein, 1997)

---

[1] The UNC shape tools are publicly available at http://www.ia.unc.edu/dev/download/shapeAnalysis.

and the size is corrected for head size variations by normalization using intracranial contents (ICC) volume. Unlike the original segmentations, the resulting SPHARM-PDM surfaces are aligned, scaling normalized, smoothed and uniformly sampled surfaces with a point-to-point correspondence, for 1002 points, defined across surfaces of different subjects.

3.4. Statistical analyses

In order to compare the shape of the caudate between SPD and control groups, we compute locally a non-parametric statistical test that compares the local surface coordinates for group mean differences at 1002 discrete surface locations. The group difference metric between the groups of surface coordinates is given by the standard robust Hotelling T^2 two sample metric. This caudate shape analysis involves computing 1002 hypothesis tests, one per surface location, and a correction for the multiple testing problem is necessary, as an uncorrected analysis is overly optimistic. Our local shape analysis employs permutation tests for the computation of the raw uncorrected p-values. Since a correction for multiple comparisons with strong control over experiment-wise type 1 errors (Pantazis et al., 2004; Styner et al., 2004) is overly pessimistic, we apply an alternative false discovery rate (FDR) based correction (Genovese et al., 2002), which results in a less conservative estimate of false-negatives. The statistical analysis provides visualizations of the group test's local effect size via mean difference magnitude displacement maps (see Fig. 3). Significance maps displaying the local statistical p-values, both raw and corrected for multiple comparisons are also generated (see
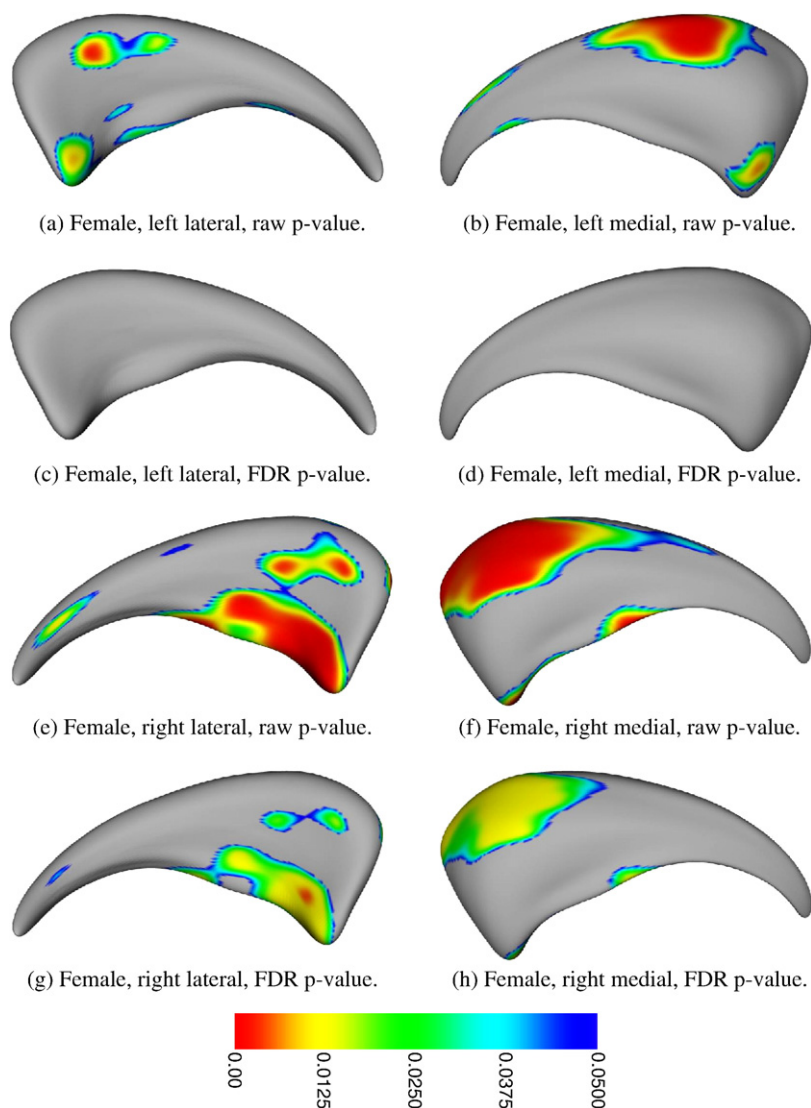

(a) Female, left lateral, raw p-value.

(b) Female, left medial, raw p-value.

(c) Female, left lateral, FDR p-value.

(d) Female, left medial, FDR p-value.

(e) Female, right lateral, raw p-value.

(f) Female, right medial, raw p-value.

(g) Female, right lateral, FDR p-value.

(h) Female, right medial, FDR p-value.

0.00   0.0125   0.0250   0.0375   0.0500

Fig. 1. Female caudate, local shape analysis results depicted on the average caudate surface. Fig. 1a,b,c,d show p value surface maps on female, left lateral and medial caudate nuclei showing patterns of significant group difference between normal and SPD female subjects using uncorrected raw data (a,b), which, however, did not survive FDR statistical correction (c,d); Fig. 1 e,f,g,h show p value surface maps on female, right lateral and medial caudate nuclei showing patterns of significant group difference between normal and SPD female subjects using uncorrected raw data (e,f) which, in large measure, survived FDR statistical correction (g,h). Colored areas indicate p values <0.05, with warmer colors showing smaller p values. Gray areas indicate p values >0.05.

Figs. 1 and 2). In addition to the local statistical shape analysis, we also compute an overall, global shape difference that summarizes the group differences across the surface via averaging. The clinical correlations were performed locally based on the rank ordering resulting from the projection of the corresponding surface points onto the line passing through the corresponding point of the average shape for all subjects in the direction perpendicular to the average surface. The rank increases in the outward direction along the surface normal. A positive correlation with respect to a chosen measure indicates that an increase in the measure coincides with structural inflation, and a negative correlation with respect to a chosen measure indicates that an increase in the measure coincides with structural deflation. Correlations were performed using a Spearman's rank order statistic. As the local correlations were performed for 1002 surface points this necessitated a correction for multiple comparisons. We used the FDR approach, with a false
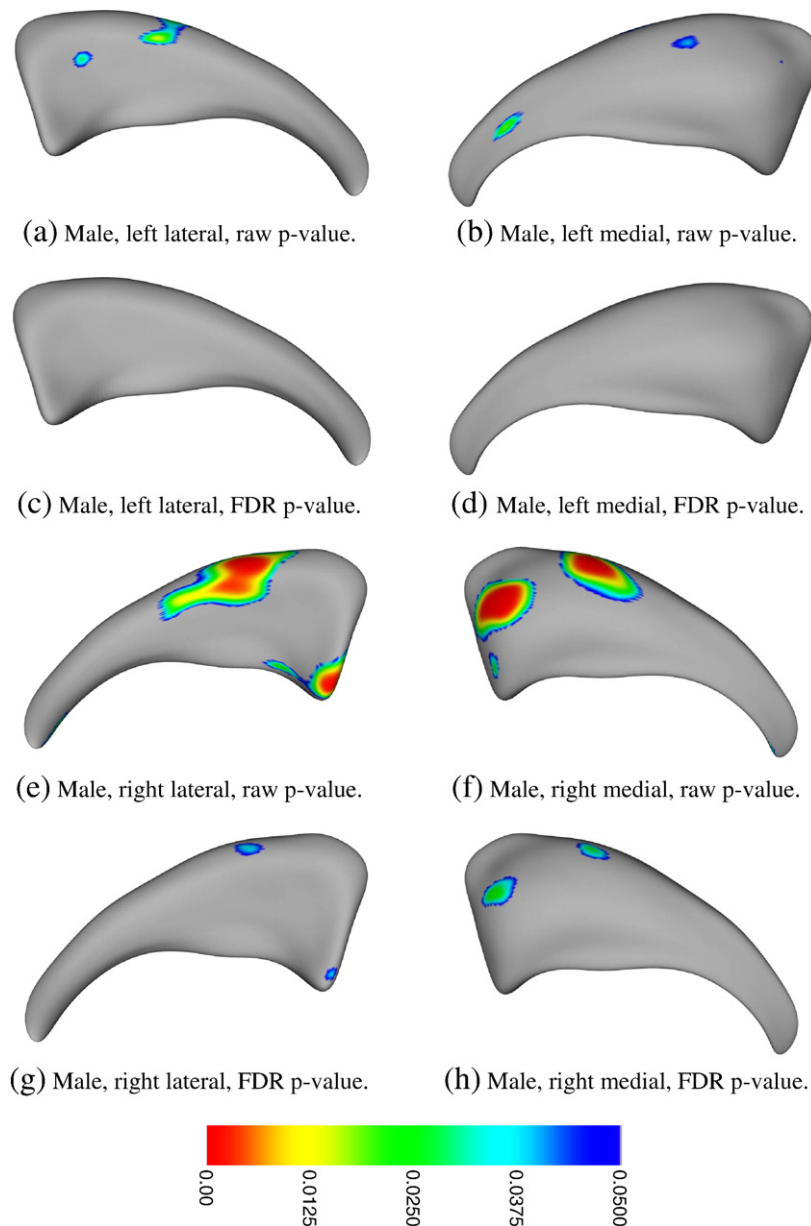

Fig. 2. Male caudate, local shape analysis results depicted on the average caudate surface: Fig. 2a,b,c,d show p value surface maps on male, left lateral and medial caudate nuclei showing patterns of significant group difference between normal and SPD male subjects using uncorrected raw data (a,b) which did not survive FDR statistical correction (c,d); Fig. 2e,f,g,h show *p* value surface maps on right male, lateral and medial caudate nuclei showing patterns of significant group difference between normal and SPD male subjects using uncorrected raw data (e,f) which, in small islets, survived FDR statistical correction (g,h). Colored areas indicate *p* values <0.05, with warmer colors showing smaller *p* values. Gray areas indicate *p* values >0.05. (For interpretation of the references to colour in this figure legend, the reader is referred to the web version of this article.)

discovery rate of 5%, which is less conservative than applying a Bonferroni correction (Genovese et al., 2002).

4. Results

4.1. Global and local shape analyses

We applied our shape analysis methodology to manually segmented caudate nuclei for both male and female data sets. All reported results were corrected for ICC volume. Here we present results based upon both raw and FDR corrected *p* value maps together with corresponding local displacement maps.

With regard to our global shape measures, which capture the average of the mean surface local differences across the whole surface, we found in male subjects a significant global surface deflation on the right ($p = 0.02$) but not the left ($p = 0.30$). Alternatively, in females, we found significant global surface deflation differences for both right ($p = 0.0042$) and left ($p = 0.044$) caudate nuclei, but more pronounced on the right.

Overall, with respect to local analyses, we found in both male and female samples: 1) more pronounced group differences in the right, versus the left, caudate nucleus, using both our raw and FDR corrected statistical tests; 2) that group differences, bilaterally, were mainly anterior, in the head of the
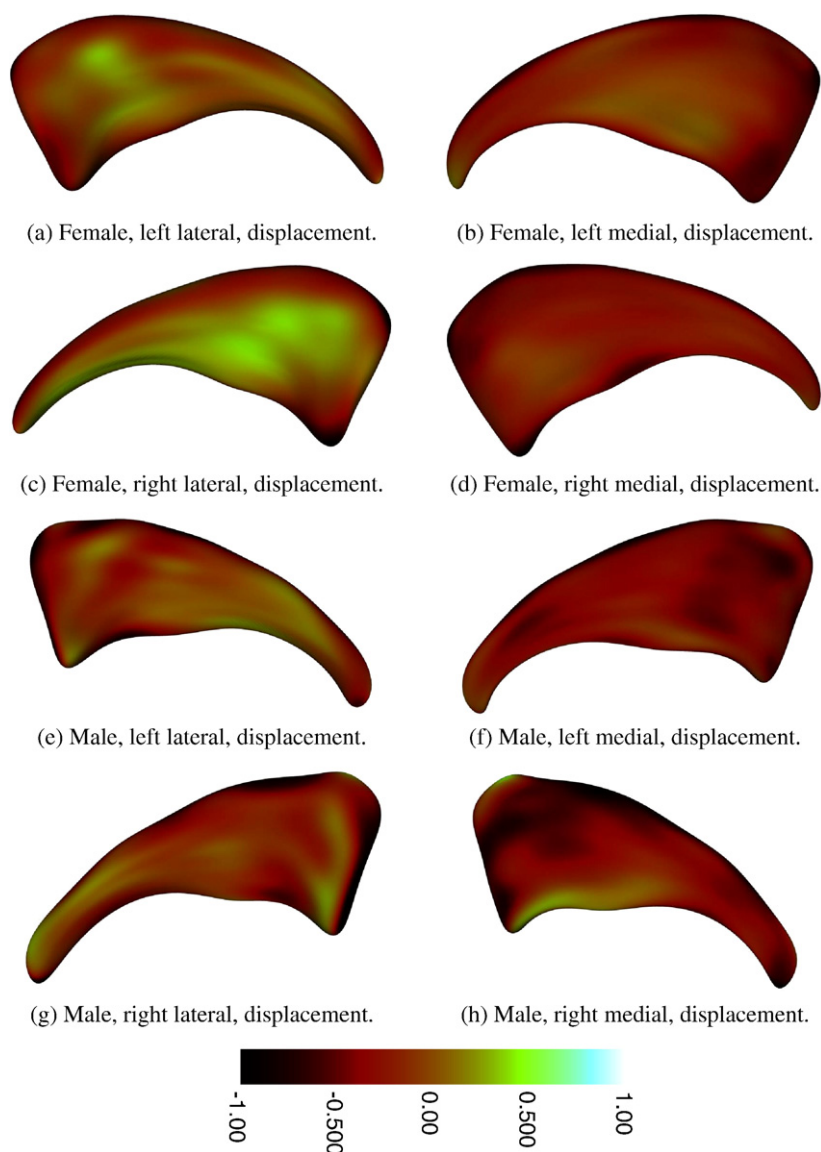

(a) Female, left lateral, displacement.

(b) Female, left medial, displacement.

(c) Female, right lateral, displacement.

(d) Female, right medial, displacement.

(e) Male, left lateral, displacement.

(f) Male, left medial, displacement.

(g) Male, right lateral, displacement.

(h) Male, right medial, displacement.

-1.00   -0.500   0.00   0.500   1.00

Fig. 3. Local displacement maps in millimeters (mm) on female and male caudate nuclei depicted on the average caudate surface: Fig. 3a,b,c,d show local displacement maps on female left and right lateral and medial caudate nuclei; Fig. 3e,f,g,h show local displacement maps on male left and right lateral and medial caudate nuclei. Colored areas indicate displacement in mm, with darker browns indicating negative mm displacement (i.e., surface deflation) for SPD subjects compared to controls, and lighter colors indicating positive mm displacement (i.e., surface inflation) for SPD compared to control subjects. (For interpretation of the references to colour in this figure legend, the reader is referred to the web version of this article.)

caudate; and 3) that no group differences survived FDR correction on the left side.

Specifically, local analyses in our female sample, based upon 28 SPD and 25 NCLs, using FDR corrected statistics, showed significant differences in the dorsal and ventral aspects of the right (Fig. 1g,h), but not left (Fig. 1c,d), head of the caudate nucleus, as revealed in our p value surface maps in Fig. 1. Further, the local displacement maps in our female subjects (Fig. 3a–d), support that these areas of significant group difference, using FDR corrected statistics, were areas where there was local caudate deflation in SPD versus NCL subjects (Fig. 3c,d).

In our male sample, local analyses, based upon 15 SPD and 14 NCLS, using FDR corrected statistics, showed small islets of significant group difference on the right head of the caudate as revealed in our p value surface maps in Fig. 2g,h. No group differences were revealed, using FDR corrected statistics, for left caudate (Fig. 2c,d). Once again, the local displacement maps in our male subjects (Fig. 3e,f,g,h) support that areas of significant difference, using FDR corrected statistics, where there was local deflation in SPD versus NCLs (Fig. 3g,h).

To further demonstrate our methodology, we present a visualization (see Fig. 4a) of the mean displacement difference, in millimeters (mm), between the mean shape, or surface, in the right medial caudate of female SPD versus female controls with a superimposed vectormap showing the direction and magnitude of the mean group displacement differences "on the surface meshes". Fig. 4b shows the covariance map of the same surfaces represented by covariance ellipsoids.

4.2. Local correlations between caudate nucleus and psychopathology in subjects with schizotypal personality disorder

Overall, our raw and FDR corrected p-value maps of correlations between local surface points and clinical measures showed that the direction of our local Spearman Rho correlations generally agreed with the direction of our prior global volume correlations for both SPD female and male subjects; that is, positive and negative global correlations resulted in positive and negative local correlations, respectively (see online Figs. 1–14, right column; http://pnl.bwh.harvard.edu/people/marc/caudateShapeAnalysis/allCaudateCorrelations.pdf). In our prior female SPD study (Koo et al., 2006), we found a positive partial correlation (controlling for age) between CVLT list A trial 5 raw scores and a trend-level correlation between list A total words learned (trials 1–5) raw scores [$p = 0.04$; $p = .051$] with total caudate relative volume; and a negative partial correlation (controlling for age) between number of nonperseverative errors on the WCST and total caudate relative volume [$p = 0.005$]. In contrast, we found no significant correlations for the control group. Moreover, assessing clinical symptoms using the SIS, we previously reported in a subset of our female SPD subjects, negative partial correlations (controlling for age) between scores of illusion, psychotic-like symptoms and sensitivity (to criticism) ($n = 15$, $p = 0.005$; $p = 0.002$; $p = 0.007$) and total caudate relative volume.

Using these same tests, in our current study, for our female SPD sample, with regard to correlations with performance on

(a) Female, right medial, displacement vectors.

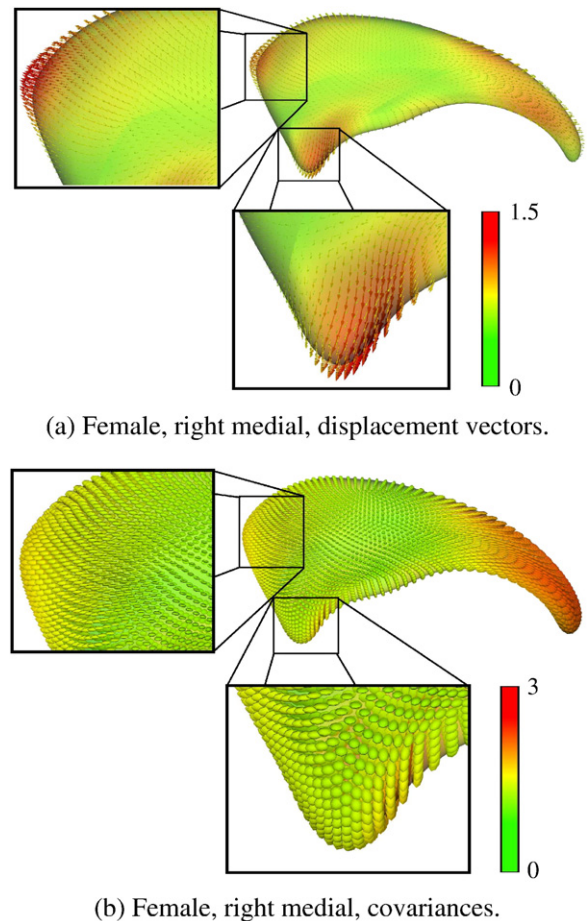
(b) Female, right medial, covariances.

Fig. 4. A color map of the right medial caudate ranging from green (0 mm difference) to red (1.5 mm difference) with a superimposed vectormap showing the direction (and magnitude) of the mean group displacement differences "on the surface meshes" between female SPD and control subjects. Vectors pointing outward indicate that the normal surface is inflated with respect to the SPD surface at that point. Overall, it can be seen that the mean shapes of the 2 groups are similar with an overall maximum difference of approximately 1.5 mm at any surface point. In Fig. 4a, we also show a zoomed view of 2 main anterior caudate regions showing large group mm displacement differences indicating surface deflation in SPD females in the right medial caudate. Fig. 4b shows the covariance map represented by covariance ellipsoids of the same right medial caudate surface for SPD compared with NCL subjects from green (0 mm^2) to red (3 mm^2); the larger the covariance ellipsoid, the greater the degree of covariance. Intuitively, one can appreciate that the 2 zoomed regions in Fig. 4a are significantly different (which the FDR corrected statistics indicated) as they represent areas both with large magnitude mm displacement differences (a more reddish hue) and relatively small covariance ellipsoids. (For interpretation of the references to colour in this figure legend, the reader is referred to the web version of this article.)

the CVLT, we found positive local significant ($n = 27$; $p < 0.05$) uncorrected correlations, bilaterally, between the degree of local inflation of surface points, primarily on the medial surface of the head of the caudate, and list A trial 5 raw scores in the CVLT. In other words, the greater the local inflation on the medial surface of the head of the caudate, the better the performance on learning new words on the 5th trial in the CVLT. Additionally, these findings, on the medial surface of the head of the caudate, were stronger for the left than for the

right caudate. Of note, these were the only *p*-value findings that survived FDR correction (see Figs 5 and 6; and note Fig. 5g and h vs Fig. 6g and h). For the other local correlations for female SPDs including the total trials 1–5 raw CVLT scores (*n* = 27) and the non-perseverative errors on the WCST (*n* = 26), local correlations again concentrated in the medial surface of the head and body of the caudate, bilaterally, and were in the predicted directions but none of these correlations survived FDR correction (see online Figs. 1,2,5,6). With regard to NCLs (*n* = 25), the local correlations with the above neuropsychological measures were generally weaker, but not always completely absent, although no local clinical correlation survived FDR correction (see online Figs. 1–6). Regarding local correlations for female SPDs for clinical

measures, due to the smaller sample size for which we had clinical measures (*n* = 13), these correlations were weaker and none survived FDR correction (see online Figs. 7–12).

In our prior male SPD study, we found bilateral negative correlations between number of perseverative errors on a delayed alternation spatial working memory task and both left and right caudate nucleus relative volume (*n* = 15, *p* = 0.03; *p* = 0.05); and, in a more lateralized pattern, negative correlations between number of perseverative errors on a verbal fluency working memory task (Levitt et al., 2002) and left, but not right, caudate nucleus relative volume (*n* = 15, *p* = 0.05; *p* = 0.09).

Using these same tests, in our current study, for our male SPD sample, local correlations with number of perseverative errors on: 1) a delayed alternation spatial working memory task; and,
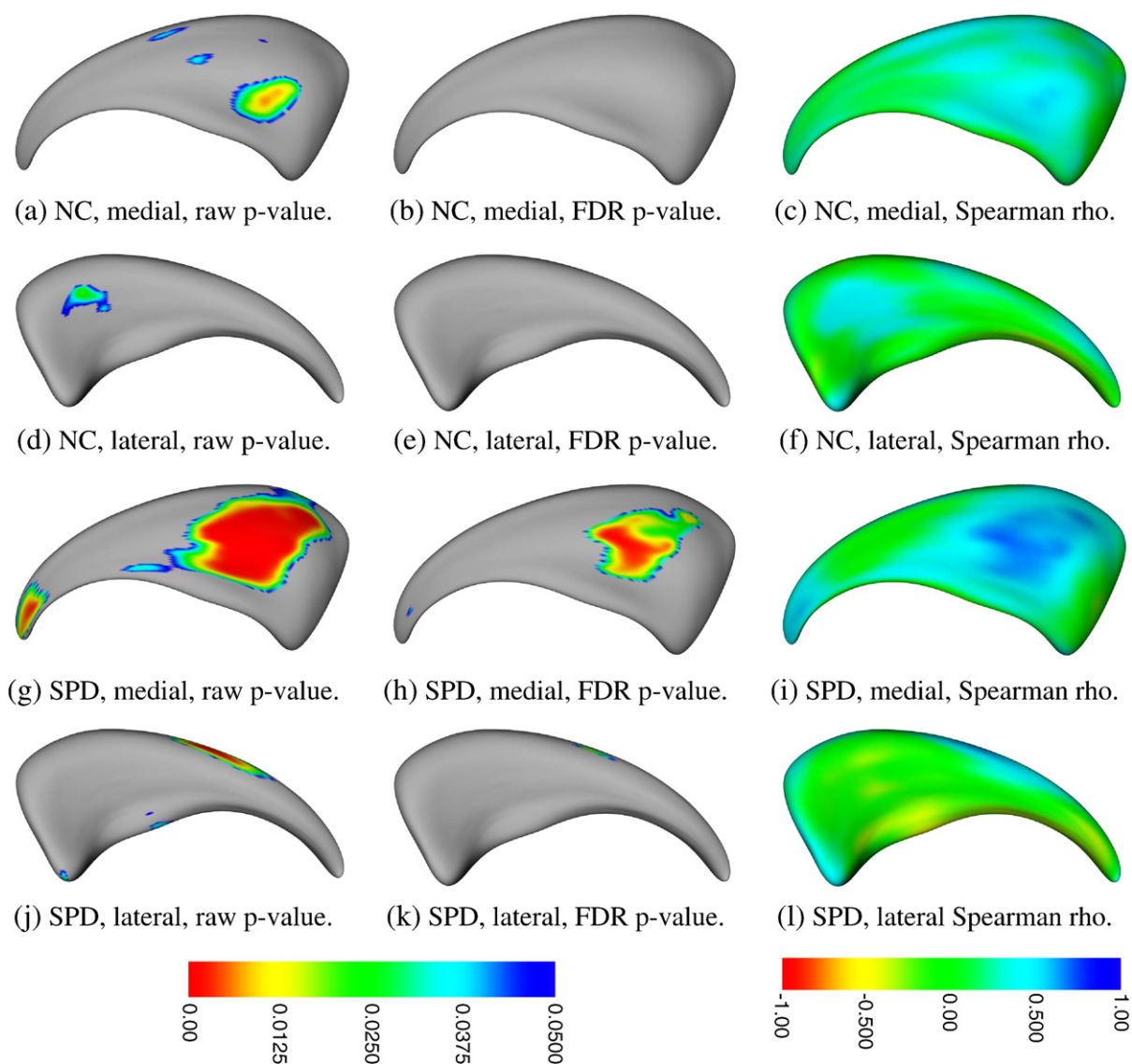

Fig. 5. Local correlations between local surface deformation and verbal learning capacity, assessed using the CVLT, in the left caudate in female SPD and NCL subjects, depicted on the average caudate surface. The left column shows the raw *p*-value, uncorrected for multiple tests. The middle column shows the *p*-value results after FDR correction for multiple comparisons. *p* values <0.05 are color coded; gray areas indicate *p* values >0.05. The right column shows the local Spearman's Rho correlation coefficients color coded for values between −1.00 to +1.00. (For interpretation of the references to colour in this figure legend, the reader is referred to the web version of this article.)
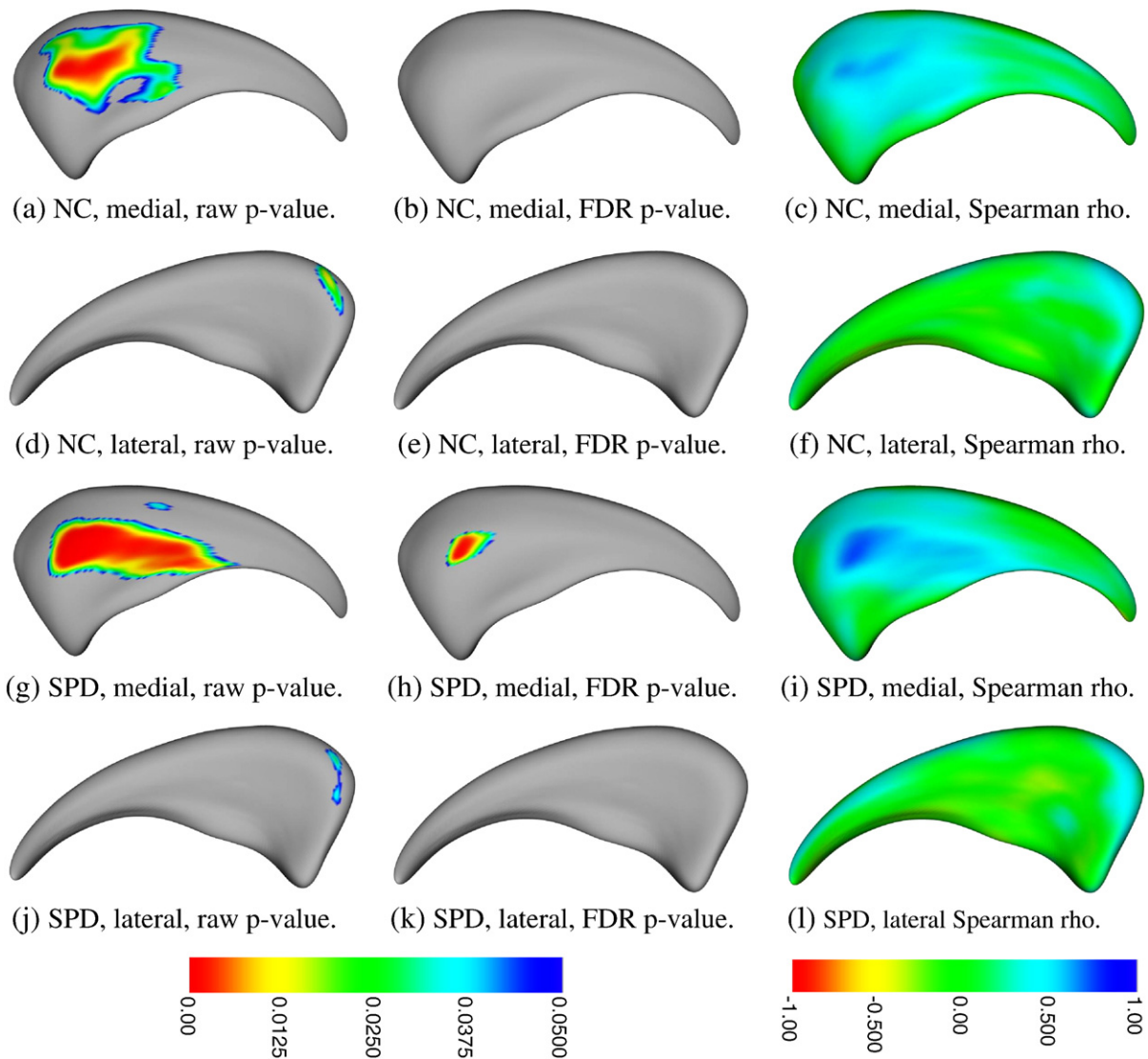
Fig. 6. Local correlations between local surface deformation and verbal learning capacity, assessed using the CVLT, in the right caudate in female SPD and NCL subjects, depicted on the average caudate surface. The left column shows the raw *p*-value, uncorrected for multiple tests. The middle column shows the *p*-value results after FDR correction for multiple comparisons. *p* values <0.05 are color coded; gray areas indicate p values.>0.05. The right column shows the local Spearman's Rho correlation coefficients color coded for values between − 1.00 to + 1.00. (For interpretation of the references to colour in this figure legend, the reader is referred to the web version of this article.)

2) a verbal fluency working memory task showed significant $(n=15; p<0.05)$ uncorrected correlations in the expected direction with greater local deflation correlating with more peserverative errors, or worse performance. These uncorrected correlations tended to be more pronounced on the medial surface of the head and body. For verbal fluency, the uncorrected correlations were more pronounced on the left than right, whereas for the delayed alternation correlations the findings were more bilateral. Again, none of these correlations survived FDR correction (see online Figs. 13–16). With regard to NCLs for male SPD subjects $(n=10$ for delayed alternation; $n=9$ for verbal fluency) there were very minimal, even uncorrected, local correlations with the above clinical measures none of which survived FDR correction (see online Figs. 13–16). Clinical local correlations for male SPD were not performed as global clinical

correlations using SANS and SAPS measures did not yield global correlations in our prior male study.

5. Discussion

The findings in our study represent the first clinical report employing the SPHARM-PDM method for shape analysis, showing both local and global group differences in the shape of the caudate in SPD subjects, and furthermore, showing clinical correlations with local shape deformation. There were several major findings. First, with regard to our global shape analyses, in the female data set both right $(p=0.0042)$ and left $(p=0.044)$ caudate nuclei showed significant global shape differences, although more pronounced on the right, whereas in the male data set, only the right caudate

($p = 0.02$) showed a significant difference. Second, with regard to our local shape analyses for both male and female subjects, we found non-uniform, lateralized group differences, which principally occurred anteriorly, in the head of the caudate. Furthermore, for our local shape analyses, we found that for both male and female subjects only the right caudate nucleus survived FDR statistical correction. Third, our local displacement maps (Fig. 3) showed that the areas of significant group difference occurred where there was local shape deflation for both our male and female SPD groups versus their respective NCL groups. Our local shape deflation, or deformation, measures compared the between group differences in the degree of local deflation/inflation at each of 1002, uniformly sampled, homologous points on the caudate surface. Lastly, fourth, we performed local caudate surface deformation correlations, performed locally based on the surface deformation with respect to the mean shape, with clinical measures for which in our prior SPD studies, we had previously found significant correlations with global caudate relative volume. Encouragingly, these local correlation results converged with our prior global results in that the direction of the correlations was in agreement. Also, of interest, the medial surface of the head of the caudate was the area of the caudate most frequently correlated with behavior. Of most importance, and not possible without a local analysis of shape, we found statistically corrected local correlations between deflated deformations in the anterior medial surface of the head of the caudate, bilaterally, and verbal learning capacity on the CVLT in female SPD. By extension, these local correlation findings implicate the specific area of the prefrontal cortex, i.e., the vmPFC, which innervates that area of the caudate.

Our findings demonstrate non-uniform, more selective deflation in anterior, versus posterior, portions of the caudate. Given the ventromedial to dorsolateral gradient for function from limbic to cognitive to motor in the striatum described by Haber and colleagues (Haber et al., 2000), our findings of more selective deflation in subregions of the anterior or head of the caudate, suggest that these SPD subjects have greater pathology in limbic and cognitive caudate compared to motor caudate. Further, our local cognitive correlation findings

which were strongest for the anterior medial surface of the caudate implicate involvement of that part of the prefrontal cortex which projects to the caudate anterior medial surface. Ongur and Price (Ongur and Price, 2000) have shown that what they describe as the 'medial' network of the orbital and medial prefrontal cortex (OMPFC) innervates selective parts of the striatum. In particular, they have shown in monkeys that the 'medial' network of the OMPFC, including the anterior cingulate cortex region (BA 25, 32 and 24), innervates selective parts of the striatum including the medial surface of the head of the caudate, but not the lateral surface (see Fig. 7). Hence, our data suggest that a selective dysfunction in the vmPFC FST subloop, of the overall FST cortical basal ganglia loops, is particularly responsible for worse behavioral performance on the CVLT verbal learning task in female SPD subjects. The perigenual prefrontal cortex, or the anterior cingulate cortex (ACC) region, has been described as being comprised of a dorsal cognitive division, and a rostral-ventral affective division. The dorsal cognitive division has been shown to be activated during various cognitive functions including verb generation in response to novel nouns, divided attention tasks and many working memory tasks (Bush et al., 2000; Devinsky et al., 1995; Fornito et al., 2004). Abnormalities in the ACC region would, thus, be expected to affect verbal learning performance adversely. For example, such abnormalities could impair the capacity to improve encoding and consolidation by the 5th learning trial in the CVLT, and thereby explain our correlation finding with this measure.

Furthermore, as discussed above, it has been proposed that SPD subjects are protected from the full-blown psychosis of chronic schizophrenia because of protective factors including reduced subcortical responsiveness of dopamine activity and more "frontal reserve capacity" (Siever and Davis, 2004). Our finding of diminished volume in the caudate nucleus if, for example it reflected reduced neuropil, with fewer dopamine receptors in striatal neurons, analogous to the reduced cortical neuropil hypothesis of Selemon and Goldman-Rakic (1999) for schizophrenia, could be interpreted as consistent with the above hypothesis of reduced subcortical dopaminergic activity in such subjects which, in
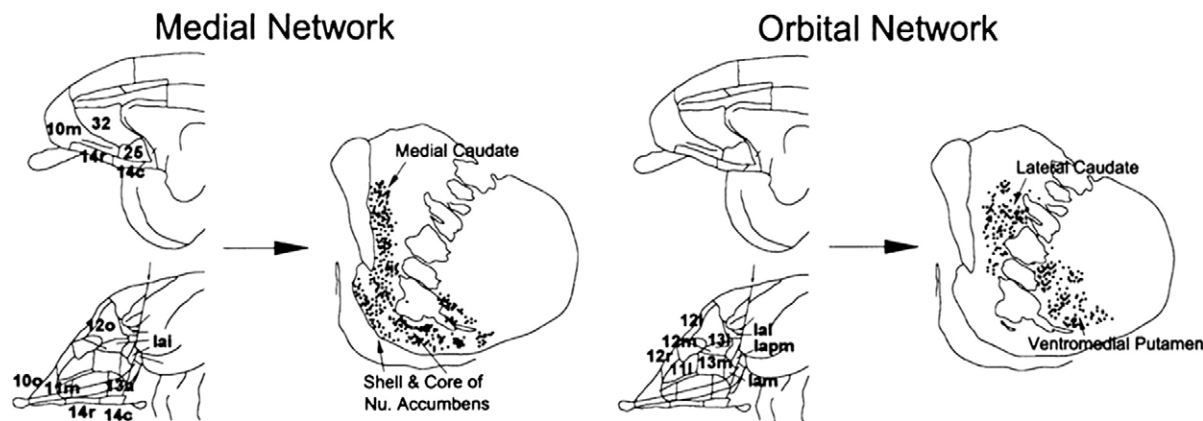

Fig. 7. Subregional distribution of projections from 'medial' and 'orbital' networks of OMPFC to the anterior, precommisural, caudate of the striatum based upon axonal tracing studies in monkeys (adapted from Ongur and Price, 2000. Reprinted with permission of Oxford University Press). Note, that the 'medial' network of OMPFC projects to the medial, but not to the lateral surface of the anterior caudate. Conversely, the 'orbital network' of OMPFC projects to the lateral, but not to the medial surface of the anterior caudate.

turn, might protect these subjects from developing the frank psychosis seen in chronic schizophrenia.

A notable strength in our subject population for this study is that our subjects were neuroleptic-naive. As it has been well established that neuroleptic medications affect caudate volume measurements (Beckmann and Lauer, 1997; Benes et al., 1985; Chakos et al., 1995; Chakos et al., 1994; Chakos et al., 1998; Corson et al., 1999b; Heckers et al., 1991; Hokama et al., 1995; Keshavan et al., 1994; Konradi and Heckers, 2001; Lauer and Beckmann, 1997; Lieberman et al., 2005; Meshul et al., 1992) our findings, hence, are not due to such effects. We note that studying SPD is not the only schizophrenia spectrum subject group which permits avoiding the confounding effect of medications on caudate volume and thus helps to discriminate whether caudate volume effects are intrinsic or secondary in schizophrenia spectrum conditions. Other subject groups which have fruitfully been studied include high risk studies of adolescents at genetic high-risk for schizophrenia, other unaffected relatives of schizophrenics and studies of first-episode (FE) psychosis subjects. In a recent high-risk study of asymptomatic, untreated young relatives (adolescent offspring) of schizophrenics, Rajarethinam et al., (2007) found smaller caudate nuclei, consistent with an intrinsic reduction in caudate volume. Conversely, Lawrie et al., (2001), in a study comparing genetically high-risk for schizophrenia young subjects with FE schizophrenic patients and controls, however, did not find any differences in caudate volume across the 3 groups. Furthermore, in a sibling study of relatives of schizophrenics, Staal et al., (2000) found that schizophrenic subjects had increased caudate volume compared to their healthy siblings and comparison subjects, but comparison subjects and siblings did not differ.

Additionally, studies have examined the striatum in neuroleptic-naïve FE schizophrenia and FE psychotic subjects, again, in an attempt to disentangle the issue of whether such volume changes are intrinsic, or not. These studies, however, have also yielded mixed results. Some studies have shown a decrease in caudate nucleus volume in neuroleptic-naive FE schizophrenics and psychotic subjects (Corson et al., 1999a; Keshavan et al., 1998). However, other studies of neuroleptic naïve FE psychotic subjects have reported no difference (Gunduz et al., 2002; Gur et al., 1998; Lang et al., 2001; Tamagaki et al., 2005). Hence, there remains controversy over the finding of decreased volume in the striatum in FE schizophrenia and psychotic subjects.

The above studies of global caudate nucleus volume in schizophrenia related conditions reveal mixed findings in neuroleptic-naive subjects. We believe that a more refined morphometric analysis such as provided by our SPHARM-PDM shape analysis provides the advantage of helping to clarify the above discrepant findings by permitting an analysis of local shape differences.

Further, our data allow for a comparison based on gender. Although, in normals, females have been reported to have relatively larger caudate volume (Filipek et al., 1994; Goldstein et al., 2001; Murphy et al., 1996), based upon our prior volume and our current shape data, it appears that both males and female SPD subjects are similar in the distribution of their morphometric deficits. Compared with their respective male and female controls, both male and female SPD subjects have bilateral caudate volume reductions together with local shape

deflation abnormalities in the caudate, which are more pronounced on the right, and more pronounced anteriorly.

A potential limitation of our study is the smaller sample size of the male SPD subjects. Hence, the clinical correlations with local shape deformation not surviving FDR correction, in our male sample, might represent a type 2 error. In support of this, when we compared the relative effect sizes for group shape difference in our male and female samples, as revealed by the local displacement maps, we found that the magnitude of millimeter displacement for both groups was very similar (see Fig. 3).

In summary, using SHPARM-PDM global and local shape analyses in neuroleptic-naïve male and female SPD subjects with bilateral caudate nucleus volume reductions, we report, both, global caudate shape group differences together with subregional, local shape deflation abnormalities in the caudate, a core component of FST circuits in the brain. Our data suggest that non-uniformly distributed shape abnormalities in the caudate nucleus in SPD are disease related and occur in both males and females. Furthermore, we show that local deflation abnormalities for both male and female SPD subjects occur particularly on the right side and principally in more anterior subregions, and that local clinical correlations both converge with global correlations and, further, specify that the strongest source of these correlations derive from the anterior medial surface of the head of the caudate. This latter finding of anterior medial caudate involvement is consistent with abnormalities in limbic and cognitive subregions of the caudate nucleus and, by extension, implicates the vmPFC, which innervates that area of the caudate. This, in turn, suggests an abnormality in the vmPFC FST subbloop of the cortical basal ganglia loops in SPD, and demonstrates the utility of local shape analysis to investigate the relationship between specific subcortical and cortical brain structures in neuropsychiatric conditions.

References

Akil, M., Kolachana, B.S., Rothmond, D.A., Hyde, T.M., Weinberger, D.R., Kleinman, J.E., 2003. Catechol-O-methyltransferase genotype and dopamine regulation in the human brain. J. Neurosci. 23, 2008–2013.

Andreasen, N.C., 1981. Scale for the Assessment of Negative Symptoms (SANS). University of Iowa, Iowa City.

Andreasen, N.C., 1984. Scale for the Assessment of Positive Symptoms (SAPS). University of Iowa, Iowa City.

Beckmann, H., Lauer, M., 1997. The human striatum in schizophrenia. II. Increased number of striatal neurons in schizophrenics. Psychiatry Res. 68, 99–109.

Benes, F.M., Paskevich, P.A., Davidson, J., Domesick, V.B., 1985. The effects of haloperidol on synaptic patterns in the rat striatum. Brain Res. 329, 265–273.

Bhatia, K.P., Marsden, C.D., 1994. The behavioural and motor consequences of focal lesions of the basal ganglia in man. Brain 117 (Pt 4), 859–876.

Bookstein, F.L., 1997. Shape and the information in medical images: a decade of the morphometric synthesis. Comput. Vis. Image Underst. 66, 97–118.

Brechbuhler, C., Gerig, G., Kubler, O., 1995. Parametrization of closed surfaces for 3-D shape description. Comput. Vis., Graphics, Image Process. 61, 154–170.

Bush, G., Luu, P., Posner, M.I., 2000. Cognitive and emotional influences in anterior cingulate cortex. Trends Cogn. Sci. 4, 215–222.

Calabresi, P., De Murtas, M., Bernardi, G., 1997. The neostriatum beyond the motor function: experimental and clinical evidence. Neuroscience 78, 39–60.

Chakos, M.H., Lieberman, J.A., Alvir, J., Bilder, R., Ashtari, M., 1995. Caudate nuclei volumes in schizophrenic patients treated with typical antipsychotics or clozapine [letter]. Lancet 345, 456–457.

Chakos, M.H., Lieberman, J.A., Bilder, R.M., Borenstein, M., Lerner, G., Bogerts, B., et al., 1994. Increase in caudate nuclei volumes of first-episode schizophrenic patients taking antipsychotic drugs. Am. J. Psychiatry 151, 1430–1436.

Chakos, M.H., Shirakawa, O., Lieberman, J., Lee, H., Bilder, R., Tamminga, C.A., 1998. Striatal enlargement in rats chronically treated with neuroleptic. Biol. Psychiatry 44, 675–684.

Corson, P.W., Nopoulos, P., Andreasen, N.C., Heckel, D., Arndt, S., 1999a. Caudate size in first-episode neuroleptic-naive schizophrenic patients measured using an artificial neural network. Biol. Psychiatry 46, 712–720.

Corson, P.W., Nopoulos, P., Miller, D.D., Arndt, S., Andreasen, N.C., 1999b. Change in basal ganglia volume over 2 years in patients with schizophrenia: typical versus atypical neuroleptics. Am. J. Psychiatry 156, 1200–1204.

Cummings, J.L., 1993. Frontal-subcortical circuits and human behavior. Arch Neurol 50, 873–880.

Delis, D.C., Kramer, J.H., Kaplan, E., Ober, B.A., 1987. California Verbal Learning Test Manual–Research Edition. Psychological Corp, San Diego.

Devinsky, O., Morrell, M.J., Vogt, B.A., 1995. Contributions of anterior cingulate cortex to behaviour. Brain 118 (Pt 1), 279–306.

Dickey, C.C., Shenton, M.E., Hirayasu, Y., Fischer, I., Voglmaier, M.M., Niznikiewicz, M.A., et al., 2000. Large CSF volume not attributable to ventricular volume in schizotypal personality disorder. Am. J. Psychiatry 157, 48–54.

Filipek, P.A., Richelme, C., Kennedy, D.N., Caviness Jr, V.S., 1994. The young adult human brain: an MRI-based morphometric analysis. Cereb. Cortex 4, 344–360.

First, M.B., Gibbon, M., Spitzer, R.L., Williams, J.B.W., Benjamin, L., 1997. Structured Clinical Interview for DSM-IV Personality Disorders (SCID-II): Interview and Questionnaire. American Psychiatric Press, Washington, DC.

First, M.B., Spitzer, R.L., Williams, J.B.W., Gibbon, M., 1995. Stuctured Clinical Interview for DSM-IV-Patient Edition (SCID-P). American Psychiatric Press, Washington, DC.

Fornito, A., Yucel, M., Wood, S., Stuart, G.W., Buchanan, J.A., Proffitt, T., et al., 2004. Individual differences in anterior cingulate/paracingulate morphology are related to executive functions in healthy males. Cereb. Cortex 14, 424–431.

Genovese, C.R., Lazar, N.A., Nichols, T., 2002. Thresholding of statistical maps in functional neuroimaging using the false discovery rate. Neuroimage 15, 870–878.

Gerig, G., Kubler, O., Kikinis, R., Jolesz, F., 1992a. Non-linear anisotropic filtering of MRI data. IEEE Trans. Med. Imaging 11, 221–232.

Gerig, G., Kubler, O., Kikinis, R., Jolesz, F.A., 1992b. Non-linear anisotropic filtering of MRI data. IEEE Trans. Med. Imaging 11, 221–232.

Gerig, G., Styner, M., 2001. Shape versus size: improved understanding of the morphology of brain structues. MICCAI 24–32.

Goldstein, J.M., Seidman, L.J., Horton, N.J., Makris, N., Kennedy, D.N., Caviness Jr., V.S., et al., 2001. Normal sexual dimorphism of the adult human brain assessed by in vivo magnetic resonance imaging. Cereb. Cortex 11, 490–497.

Gunduz, H., Wu, H., Ashtari, M., Bogerts, B., Crandall, D., Robinson, D.G., et al., 2002. Basal ganglia volumes in first-episode schizophrenia and healthy comparison subjects. Biol. Psychiatry 51, 801–808.

Gur, R.E., Maany, V., Mozley, P.D., Swanson, C., Bilker, W., Gur, R.C., 1998. Subcortical MRI volumes in neuroleptic-naive and treated patients with schizophrenia. Am. J. Psychiatry 155, 1711–1717.

Haber, S.N., Fudge, J.L., McFarland, N.R., 2000. Striatonigrostriatal pathways in primates form an ascending spiral from the shell to the dorsolateral striatum. J. Neurosci. 20, 2369–2382.

Heaton, R.K., 1981. Wisconsin Card Sorting Test Manual. Psychological Assessment Resources, Odessa.

Heckers, S., Heinsen, H., Heinsen, Y., Beckmann, H., 1991. Cortex, white matter, and basal ganglia in schizophrenia: a volumetric postmortem study. Biol. Psychiatry 29, 556–566.

Hokama, H., Shenton, M.E., Nestor, P.G., Kikinis, R., Levitt, J.J., Metcalf, D., et al., 1995. Caudate, putamen, and globus pallidus volume in schizophrenia: a quantitative MRI study. Psychiatry Res. 61, 209–229.

Kendler, K.S., Lieberman, J.A., 1989. The Structured Interview for Schizotypy (SIS): a preliminary report. Schizophr. Bull. 15, 559–571.

Kendler, K.S., McGuire, M., Gruenberg, A.M., O'Hare, A., Spellman, M., Walsh, D., 1993. The Roscommon Family Study. I. Methods, diagnosis of probands, and risk of schizophrenia in relatives. Arch Gen Psychiatry 50, 527–540.

Keshavan, M.S., Bagwell, W.W., Haas, G.L., Sweeney, J.A., Schooler, N.R., Pettegrew, J.W., 1994. Changes in caudate volume with neuroleptic treatment [letter]. Lancet 344, 1434.

Keshavan, M.S., Rosenberg, D., Sweeney, J.A., Pettegrew, J.W., 1998. Decreased caudate volume in neuroleptic-naive psychotic patients. Am. J. Psychiatry 155, 774–778.

Konradi, C., Heckers, S., 2001. Antipsychotic drugs and neuroplasticity: insights into the treatment and neurobiology of schizophrenia. Biol. Psychiatry 50, 729–742.

Koo, M.S., Levitt, J.J., McCarley, R.W., Seidman, L.J., Dickey, C.C., Niznikiewicz, M.A., et al., 2006. Reduction of caudate nucleus volumes in neuroleptic-naive female subjects with schizotypal personality disorder. Biol. Psychiatry.

Lang, D.J., Kopala, L.C., Vandorpe, R.A., Rui, Q., Smith, G.N., Goghari, V.M., et al., 2001. An MRI study of basal ganglia volumes in first-episode schizophrenia patients treated with risperidone. Am. J. Psychiatry 158, 625–631.

Lauer, M., Beckmann, H., 1997. The human striatum in schizophrenia. I. Increase in overall relative striatal volume in schizophrenics. Psychiatry Res. 68, 87–98.

Lawrie, S.M., Whalley, H.C., Abukmeil, S.S., Kestelman, J.N., Donnelly, L., Miller, P., et al., 2001. Brain structure, genetic liability, and psychotic symptoms in subjects at high risk of developing schizophrenia. Biol. Psychiatry 49, 811–823.

Levitt, J.J., McCarley, R.W., Dickey, C.C., Voglmaier, M.M., Niznikiewicz, M.A., Seidman, L.J., et al., 2002. MRI study of caudate nucleus volume and its cognitive correlates in neuroleptic-naive patients with schizotypal personality disorder. Am. J. Psychiatry 159, 1190–1197.

Levitt, J.J., Westin, C.F., Nestor, P.G., Estepar, R.S., Dickey, C.C., Voglmaier, M.M., et al., 2004. Shape of caudate nucleus and its cognitive correlates in neuroleptic-naive schizotypal personality disorder. Biol. Psychiatry 55, 177–184.

Lieberman, J.A., Tollefson, G.D., Charles, C., Zipursky, R., Sharma, T., Kahn, R.S., et al., 2005. Antipsychotic drug effects on brain morphology in first-episode psychosis. Arch. Gen. Psychiatry 62, 361–370.

Meshul, C.K., Janowsky, A., Casey, D.E., Stallbaumer, R.K., Taylor, B., 1992. Effect of haloperidol and clozapine on the density of "perforated" synapses in caudate, nucleus accumbens, and medial prefrontal cortex. Psychopharmacology (Berl) 106, 45–52.

Murphy, D.G., DeCarli, C., McIntosh, A.R., Daly, E., Mentis, M.J., Pietrini, P., et al., 1996. Sex differences in human brain morphometry and metabolism: an in vivo quantitative magnetic resonance imaging and positron emission tomography study on the effect of aging. Arch. Gen. Psychiatry 53, 585–594.

Ongur, D., Price, J.L., 2000. The organization of networks within the orbital and medial prefrontal cortex of rats, monkeys and humans. Cereb. Cortex 10, 206–219.

Pantazis, D., Leahy, R.M., Nichols, T.E., Styner, M., 2004. Statistical surface-based morphometry using a non-parametric approach. IEEE Int. Symp. Biomed. Imaging (ISBI) 1283–1286.

Rajarethinam, R., Upadhyaya, A., Tsou, P., Upadhyaya, M., Keshavan, M.S., 2007. Caudate volume in offspring of patients with schizophrenia. Br. J. Psychiatry 191, 258–259.

Seidman, L.J., Faraone, S.V., Goldstein, J.M., Goodman, J.M., Kremen, W.S., Matsuda, G., et al., 1997. Reduced subcortical brain volumes in nonpsychotic siblings of schizophrenic patients: a pilot magnetic resonance imaging study. Am. J. Med. Genet. 74, 507–514.

Selemon, L.D., Goldman-Rakic, P.S., 1999. The reduced neuropil hypothesis: a circuit based model of schizophrenia. Biol. Psychiatry 45, 17–25.

Shenton, M.E., Gerig, G., McCarley, R.W., Szekely, G., Kikinis, R., 2002. Amygdala-hippocampal shape differences in schizophrenia: the application of 3D shape models to volumetric MR data. Psychiatry Res. 115, 15–35.

Shihabuddin, L., Buchsbaum, M.S., Hazlett, E.A., Silverman, J., New, A., Brickman, A.M., et al., 2001. Striatal size and relative glucose metabolic rate in schizotypal personality disorder and schizophrenia. Arch. Gen. Psychiatry 58, 877–884.

Siever, L.J., Davis, K.L., 2004. The pathophysiology of schizophrenia disorders: perspectives from the spectrum. Am. J. Psychiatry 161, 398–413.

Siever, L.J., Kalus, O.F., Keefe, R.S., 1993. The boundaries of schizophrenia. Psychiatr. Clin. North Am. 16, 217–244.

Staal, W.G., Hulshoff Pol, H.E., Schnack, H.G., Hoogendoorn, M.L., Jellema, K., Kahn, R.S., 2000. Structural brain abnormalities in patients with schizophrenia and their healthy siblings. Am. J. Psychiatry 157, 416–421.

Styner, M., Lieberman, J., Pantazis, D., Gerig, G., 2004. Boundary and medial shape analysis of the hippocampus in schizophrenia. Med. Image Anal. 8, 197–203.

Styner, M., Lieberman, J.A., McClure, R.K., Weinberger, D.R., Jones, D.W., Gerig, G., 2005. Morphometric analysis of lateral ventricles in schizophrenia and healthy controls regarding genetic and disease-specific factors. Proc. Natl. Acad. Sci. U S A 102, 4872–4877.

Styner, M., Oguz, I., Xu, S., Brechbuhler, C., Pantazis, D., Levitt, J.J., et al., 2006. Framework for the statistical shape analysis of brain structures using SPHARM-PDM. Insight J. 1–21.

Tamagaki, C., Sedvall, G.C., Jonsson, E.G., Okugawa, G., Hall, H., Pauli, S., et al., 2005. Altered white matter/gray matter proportions in the striatum of patients with schizophrenia: a volumetric MRI study. Am. J. Psychiatry 162, 2315–2321.

Weinberger, D.R., 1987. Implications of normal brain development for the pathogenesis of schizophrenia. Arch. Gen. Psychiatry 44, 660–669.

Wells, W., Kikinis, R., Grimson, W., Jolesz, F.A., 1996. Adaptive segmentation of MRI data. IEEE Trans. Med. Imaging 15, 429–442.